

Cho C, Elias A, Batcheller J, Dolez P, Chung H-J. Electrical conduction of reduced graphene oxide coated meta-aramid textile and its evolution under aging conditions. *Journal of Industrial Textiles*. 50(8), 1330-1347, 2021. Copyright © 2021 (Sage Publications).DOI: 10.1177/1528083719869387

Electrical conduction of reduced graphene oxide coated meta-aramid textile and its evolution under aging conditions

Chungyeon Cho[†], Anastasia L. Elias [†], Jane Batcheller[‡], Patricia Dolez^{*,‡}, Hyun-Joong Chung^{*,†}

[†]Department of Chemical and Materials Engineering, University of Alberta, Edmonton, Alberta T6G1H9, Canada

[‡]Department of Human Ecology, University of Alberta, Edmonton, Alberta T6G 2N1, Canada

* Address correspondence to E-mails: pdolez@ualberta.ca , chung.hj13@ualberta.ca

Abstract:

High-performance textiles – such as those used in protective clothing – age silently, undergoing a gradual reduction in their protective properties. We propose that an electrically conducting layer that loses its conductivity systematically under aging conditions can be used as an end-of-life-sensor for textiles. In the present work, we first present a simple method to prepare conductive tracks on a meta-aramid woven fabric using reduced graphene oxide (rGO). While 15 iterations of rGO coating cycles were needed to wrap around each m-aramid fiber with rGO sheets completely, 10 cycles were sufficient to establish the electrical conductivity that remained stable for up to 10 laboratory wash cycles (equivalent to 50 domestic laundry cycles). The conductivity of these rGO

coated fabrics remained stable upon immersion in water. Furthermore, we established a fabrication protocol for patterning both single-sided and two-sided rGO tracks on the m-aramid fabric. The former is designed to lose its conductivity upon abrasion, while the latter is designed to undergo a gradual transition in properties during aging. Assessment with a Martindale abrasion tester revealed that the single-sided rGO-track lose its conductivity after 150 abrasion cycles, whereas the two-sided rGO-tracks survived 3000 abrasion cycles. These results demonstrate that a simple rGO coating technique can be used to prepare end-of-life sensors for high-performance textiles.

Keywords: meta-aramid fabric, end-of-life sensor, reduced graphene oxide, conductive textile patterning, launderability, abrasion resistance

1. Introduction

High-performance fibers are used for personal protective equipment for workers exposed to heat and fire, cold temperatures, mechanical hazards, and electric arcing [1]. In addition, these high-performance fibers are used in the automotive and aerospace industries, among others. However, these fibers may gradually lose their performance as a result of exposure to various environmental factors (heat, UV, humidity, abrasion, etc.). In fact, studies done on used firefighter protective garments, some retired and some still in service, have shown significant reductions in both mechanical performance and resistance to water penetration [2]. Large losses in the mechanical performance of fire resistant fabrics made with these high performance fibers were also observed using accelerated thermal [3,4], UV [5], and moisture [6] aging programs. Therefore, monitoring the aging process of these high-performance fibers/fabrics is critical. Still, although significant efforts have been devoted towards this goal over the last 20 years [7], there is currently no *non-destructive* test method that enables assessment of the residual performance of these fabrics as a result of aging [8]. End users may use perceivable physical alterations, such as visible wear or discoloration, as an indicator; however some fabrics used for firefighters' protective clothing exposed either to radiant or convective heat were reported to undergo a reduction in mechanical strength of 40 to 79% before a discoloration could be detected [4]. Other aging monitoring strategies, e.g. using sensors, should thus be explored to help ensure the safety and function of these materials.

Graphenic nanomaterials offer interesting properties that can be applied in the development of sensors for textiles [9]. One potential application is to implement textile-based wearable electronic devices (e-textiles) in which patterned graphenic nanomaterials act as conductive traces between various components. Because of hydroxyl and carboxylic functional groups in the

graphenic nanomaterials, a good bonding is obtained with fabrics and can lead flexible, washable, and wearable e-textiles [10-15].

In order to establish electrical connections between active device components, various textile manufacturing techniques, including embroidery [16], weaving [17], knitting [18], screen inkjet printing [15] and yarn coating [19], have been suggested. Among these techniques, the yarn coating method is a low-complexity process because it utilizes a finished fabric without requiring specialized printing equipment. For instance, textile electrical components have largely been produced by simply coating textiles with metals or conductive polymers [20]. Recently, graphene-coated textiles have generated much interest due to the ease of the coating and reducing process [20,21]. In particular, the “dip and dry” method and further reduction with ascorbic acid has been adopted for conventional reduced graphene oxide (rGO) coating fabrication [23-25]. For schematic illustration of the coating mechanism, interested readers may refer to Figure 1 in Ref [23] and Figure 1 in Ref [25].

In this study, we investigated the production of conductive tracks on fire protective fabrics using rGO coatings. The stability of the rGO tracks was studied following exposure to water immersion, laundering, and abrasion. The ultimate objective is to produce graphene-based end-of-life sensors for fire protective fabrics.

2. Experimental

2.1 Materials

The fabric used in this study is a woven meta-aramid fabric (weave: 2/1 twill; mass: 222 g/m²; fabric count: 31 warp x 26 weft yarns/cm; thickness: 0.38 mm). In order to investigate the scouring

effect on the graphene coating process, the fabric was used as received as well as after being subjected to a pre-washing treatment involving 50 washing/drying cycles according to Procedure III E (50°C, tumble dry) of CAN/CGSB 4.2 No 58 [26].

The graphene oxide (GO) solution (4 mg/mL) was purchased from Graphenea, Spain. L-ascorbic acid (L-AA) from Sigma-Aldrich (Oakville, ON, Canada) was used as a reducing agent for graphene oxide. 2-propanol (IPA) was purchased from Sigma-Aldrich (Oakville, ON, Canada).

2.2 Preparation of the rGO coated m-aramid fabric

The m-aramid fabric (as-received or pre-washed) was cut into 2 cm x 2 cm pieces with a laser cutter (Versalaser Engraver, ULS, AZ, USA). The specimens were cleaned using deionized (DI) water and IPA, and dried at 65°C for 15 min. The specimens were then dipped into 10 mL of graphene oxide solution for 15 min and dried at 65 °C for 30 min. This “dip and dry” coating procedure was repeated to obtain different add-on masses of rGO coating on the fabric specimens (1, 5, 10, and 15 dips). Between each rGO coating, the dry specimens were reduced by immersion in 40 mg/mL of L-AA at 90 °C for 4 h. They were then rinsed with DI water and IPA, and placed in an oven (Symphony-VWR, Vacuum brand 2 C) at 80°C for 30 min. An illustration of the rGO coating process on the m-aramid fabric specimen is provided in Fig. 1. Except for the results shown in Fig. 3, the specimens were exfoliated with adhesive tape at the end of each dip-dry-reduce cycle in order to remove the rGO flakes not firmly attached to the fabric substrate.

The rGO add-on ratio can be calculated using equation (1):

$$\text{Add-on ratio} = \frac{m_n - m_0}{m_0} \times 100 \quad (1)$$

where m_0 is the mass of the uncoated fabric specimen and m_n is the mass of “n”-time rGO-coated fabric specimen.

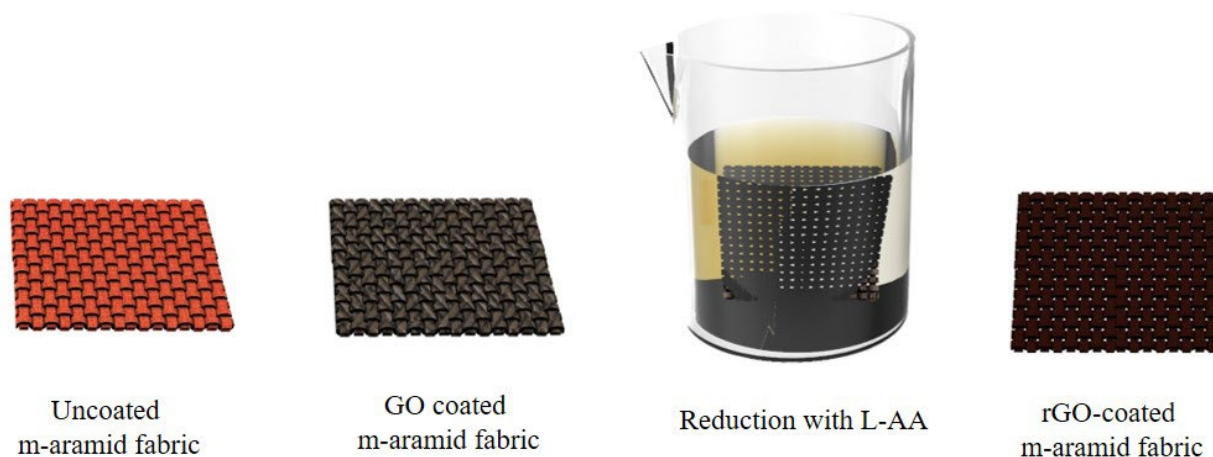


Fig. 1 Scheme of rGO coating process on m-aramid fabric.

2.3. Preparation of rGO tracks on the m-aramid fabric

To pattern rGO on a single side of the fabric specimen, a 3-inch diameter wax film was first printed on a polyethylene terephthalate (PET) film by wax printer (ColorQube 8570, Xerox). The printed wax pattern was transferred to the back side of the fabric specimen using a Bench Top Standard Heated Press (Carver, Inc, IN, USA) at 65 °C for 5 min, as illustrated in Fig. 2(a); this wax layer protected the back surface of the fabric during subsequent processing. Then, the wax-transferred fabric specimen was sandwiched between two round acrylic molds, one solid and the other bearing three tracks (with dimensions of 1.5 cm × 3 cm, (width, length, respectively)). The mold with the tracks was positioned on the face side of the fabric, i.e. the side without the wax film. Fig. 2(b) shows the detail of the rGO-patterning process.

Once the molds were in place, 200 μ L of GO solution was deposited onto the front side of fabric, and heat-pressure-transferred wax layer on backside acted as a mask, which was localizing the GO solution in the patterned area. The specimen was left for 30 min in an oven at 65 °C to dry specimen. After drying, the GO-tracks were reduced by immersion in 40 mg/mL L-AA solution at 90 °C for 4 h. After reduction, loose rGO was exfoliated with adhesive tape as described in section

2.2. This process of coating, drying, reducing, and exfoliating the rGO comprises one coating cycle and was repeated 15 times. The heat-pressure-transferred wax layer remained intact with well-defined features over all 15 coating cycles; no blurring was observed in the rGO pattern.

To prepare rGO tracks on both sides of the fabric specimens, the rGO patterning process was conducted by sandwiching the fabric between two acrylic molds bearing the three rectangular tracks. Great care was taken to ensure that the position of the tracks in the two molds corresponds. 200 μL of GO solution was used to pattern the tracks on both sides of the fabric, with a 30 min at 65 $^{\circ}\text{C}$ drying period between each side. The rest of the process was similar to what was used to prepare the single-sided tracks, including the number of coating cycles applied.

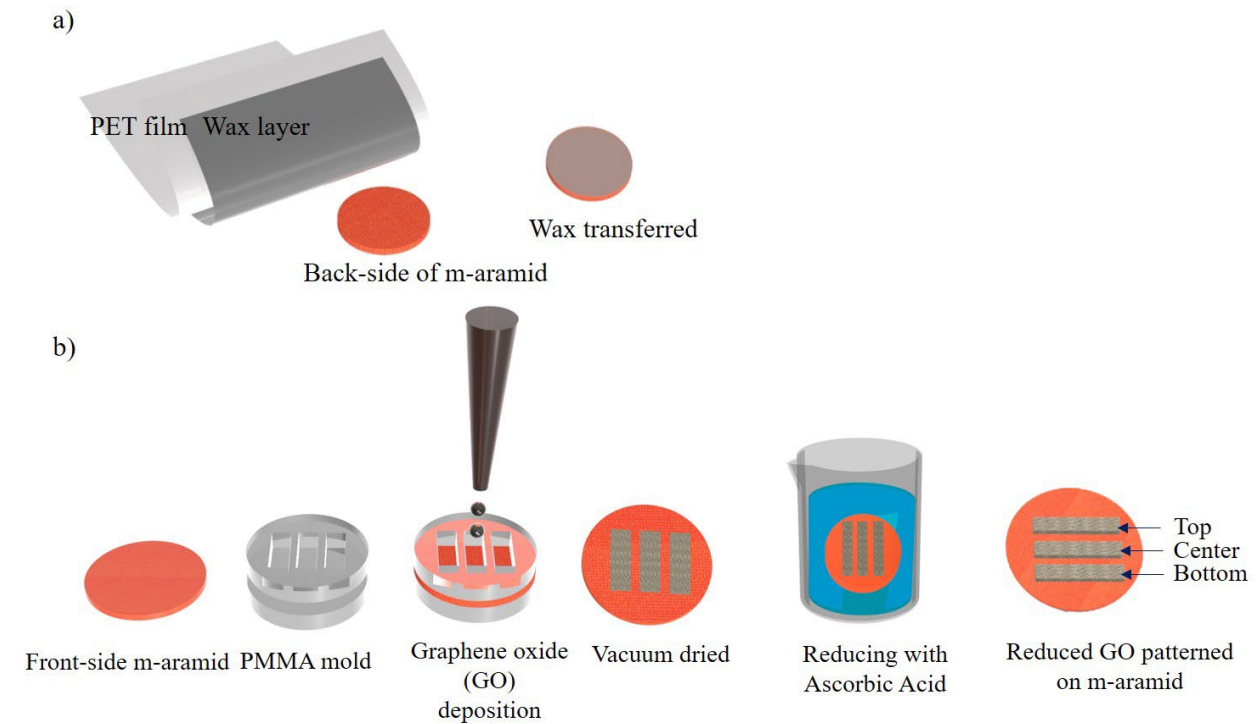


Fig. 2 Scheme of rGO patterning on fabric specimen (a) Wax layer deposition, (b) Patterning and reduction process.

2.4 Specimen general characterization

The surface morphological details of the rGO-coated textile were observed by a field emission scanning electron microscope (FE-SEM, Zeiss Sigma) and Helium Ion Microscope (HIM) (Zeiss Orion NanoFab, Zeiss Sigma). The sheet resistance (R_s) of the rGO-coated textile was measured using a 4-point-probe (Pro4 4000, Lucas Labs, CA, USA). Three measurements were made for each specimen/condition, and the results were averaged.

The electrical resistance of the rGO-tracks was measured with a digital multimeter (Fluke 77-4 Industrial Multimeter, NC, USA). Three measurements were carried out on each rGO track, and the results were averaged. A piece of adhesive conductive silver strip was installed on each end of the rGO track. The measurement of the electrical resistance of the rGO-track was conducted by connecting the digital multimeter between the conductive silver strips under the assumption that the resistance of the silver conductive strips and the contact resistance with the rGO track is negligible compared to the resistance of the rGO track itself.

2.5 Washing fastness of the rGO-coated fabric

Tests were conducted to assess the effect of repeated laundering on the electrical conductivity of the rGO tracks on the fabric. Accelerated washing was performed with a Launder-Ometer (Atlas, IL, USA) following the ISO 105-C06 standard and test procedure A1M [27]. One cycle of accelerated washing using the Launder-Ometer is equivalent to 5 cycles of domestic laundering. According to this standard, 150 mL of washing solution prepared with 4 g/L of detergent was used to wash the specimens with 10 steel balls at 40 °C. Three specimens were collected from the canister after a predetermined number of washing cycles (1, 3, 5, 7, 9, and 10 cycles), where each cycle lasted 6 min. Immediately after being collected, the specimens were rinsed with DI water and dried at 65 °C for 15 min. Then, the R_s value was measured on each of the three replicates.

The surface morphology of the rGO-coated fabric (before and after the different number of washing cycles) was observed by scanning electron microscope.

2.6 Martindale abrasion resistance test of the rGO-coated fabric

The resistance of the rGO coatings to wear was assessed by submitting the specimens to abrasion cycles using a Martindale abrasion tester and then measuring the residual electrical conductivity. The abrasion test was carried out with a M235 Martindale Abrasion Tester (SDL Atlas, Rock Hill, SC, USA) following the ASTM D4966 standard [28]. In accordance with the standard, the rGO-coated fabric specimens were abraded using standard wool abrasant fabric with a 47.5 rpm abrading speed. In order to accommodate the small size of the specimens, they were mounted on the three top (mobile) fabric holders while the wool abrasant fabric was installed on the bottom (stationary) fabric holders. After a defined number of cycles, the abrasion tester was stopped, the specimen was removed from its holder, and the specimen's electrical conductivity was measured. Then, the specimen was mounted again on the specimen holder for another series of cycles. The test was conducted on specimens bearing single- and double-sided rGO tracks.

2.7 Water immersion resistance of the rGO-coated fabric

The resistance of the rGO-coated fabric to water immersion was assessed by measuring the electrical resistance R_s of the specimens after a 24 h immersion in DI water at room temperature followed by 30 min drying at 65 °C in an oven. The 24 h immersion was repeated 5 times on each specimen, for a total of 120 h.

2.8 Statistical Analysis

Measurements were generally performed 3 times, and average values and standard deviations are reported. Where applicable, statistical significance was evaluated using the ANOVA analysis.

3. Results and discussion

3.1 Effect of rGO-coating conditions

As the initial fabric condition may affect the rGO-coating performance, trials were conducted using the m-aramid fabric in two conditions: as-received and pre-washed (see procedure in Section 2.1). Pre-washing is considered a scouring process as it removes non-permanent textile finishes and other impurities from the surface of the as-received fabric [29]. The removal of strongly hydrophobic contaminants from the surface of the fabric may enhance its affinity for GO, but may also create a rougher surface which is harder to coat with a small number of layers. Fig. 3 shows the variation in the rGO coating sheet resistance as a function of the number of coating cycles for the two initial conditions of the fabric. When collecting this data, no exfoliation was applied between the coating cycles. For each type of fabric, an increase in the number of coating cycles – and correspondingly the amount of rGO deposited – led to a reduction in the rGO sheet resistance.

Fig.3 also showed markedly different R_s values up to the 2nd rGO coating for the as-received and pre-washed fabric conditions: the rGO coating on the pre-washed m-aramid initially had a lower R_s than the rGO coating on the as-received fabric. This indicates that the washing treatment was effective at improving the GO affinity and bonding with the m-aramid fibers. The difference in R_s between the two initial fabric conditions disappeared after the 2nd rGO coating cycle. This implies that two coating cycles were sufficient to coat the m-aramid fibers at the surface of the fabric with rGO sheets. Further coating cycles added new GO layers on top of the underlying

rGO layers, i.e. without any contact with the m-aramid fabric. This can be evidenced by the lower drop in the rGO coating sheet resistance and the absence of significant difference between the as-received and pre-washed conditions after the 3rd coating cycle (see inset in Fig. 3). After 15 coating cycles, the sheet resistance of the rGO coating on the m-aramid fabric reached a value in the range of 10 Ω/\square . As a comparison, the sheet resistance of uncoated m-aramid fabric is more than 10^{16} Ω/\square [29].

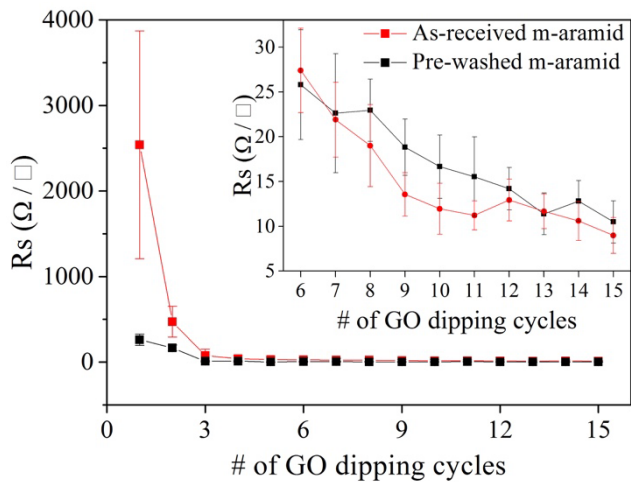


Fig. 3 Sheet resistance (R_s) of rGO coating as a function of the number of coating cycles (including coating, drying, and reduction, but without the exfoliation step) for the two initial conditions of the m-aramid fabric, as-received and pre-washed (Inset: scale-up of the low resistance part of the curve)

The left column of Fig. 4 shows FE-SEM images of the rGO-coated m-aramid fabric after 5, 10, and 15 successive coating cycles without the exfoliation step. With successive rGO coatings, the shape of the fibers becomes less and less pronounced, suggesting that the rGO sheets first covered the m-aramid fibers and then built up in layers; after the 15th rGO coating (Fig. 4(c)), the fibers are no longer visible as the rGO has created a smooth surface layer. However, these stacked rGO layers would likely be easily damaged when the fabric is bent or folded (the large crack in the middle of Fig. 4(c) may have resulted from mechanical deformation). In addition, the images of the layers produced without exfoliation suggests the presence of a number of loosely attached

rGO sheets on the fabric surface. Ideally, the rGO layers should not cover the entire fabric surface but should wrap around the individual fibers. Consequently, the coating process was modified to include an rGO exfoliation step between each coating cycle (see Section 2.2). The right column of Fig. 4 shows FE-SEM images of the rGO-coated m-aramid fabric (after 5, 10, and 15 successive coating cycles) with this added exfoliation step. These specimens were prepared using the as-received fabric. A comparison between left and right column of Fig. 4 shows that for the coatings prepared with the exfoliation step, rGO sheets appear to wrap around the individual m-aramid fibers and the number of loosely attached graphene sheets is strongly reduced. The HIM image in Fig. 5 illustrates that the rGO sheets completely and conformally cover the surface of individual m-aramid fibers. Here, a stark contrast is achieved between insulating (m-aramid) and conducting (rGO) components as HIM imaging is free from charging-inflicted artefacts in the insulating regions.

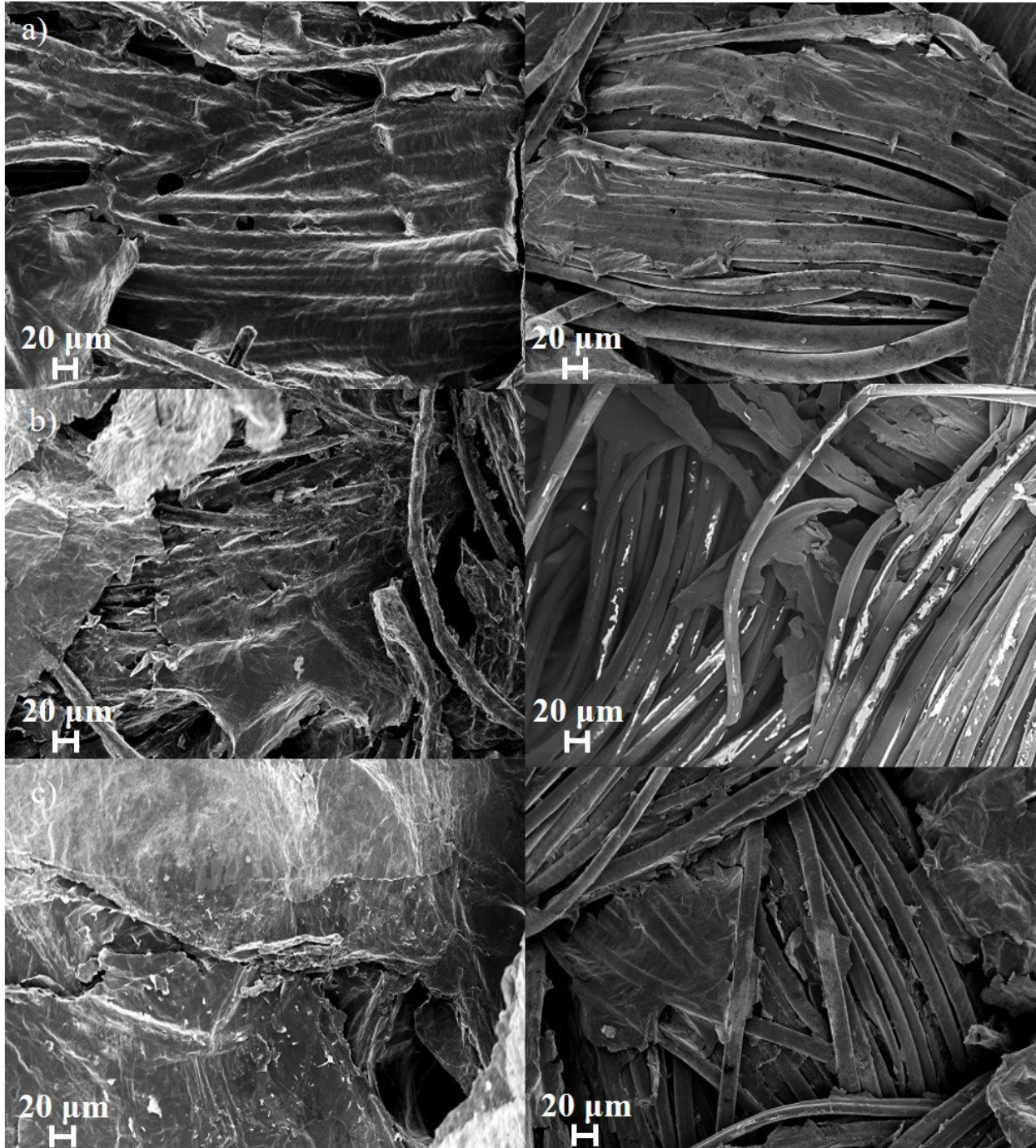


Fig. 4 FE-SEM images of rGO coating on as-received m-aramid fabric prepared (left column) without and (right column) with the exfoliation step. Samples were imaged after a) 5th rGO coating, b) 10th rGO coating, and c) 15th rGO coating.

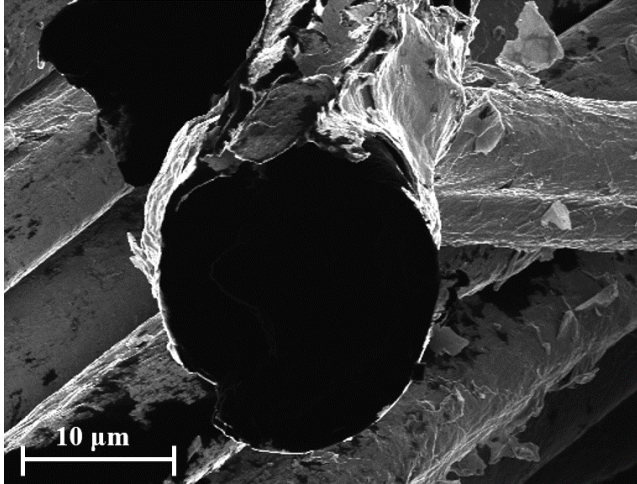


Fig. 5 Helium-ion microscope (HIM) image of rGO wrapped individual m-aramid fiber. The black hole in the center of the image corresponds to the uncoated cross-section of the fiber.

The rGO add-on ratio as a function of the number of rGO coating cycles is shown in Fig. 6. The specimens were prepared using the as-received m-aramid fabric. The specimen preparation included the added exfoliation step after the rGO reduction step. It is observed that the rGO add-on percentage increases with the increasing number of rGO coating cycles. The rGO add-on ratio was $9 (\pm 1) \%$ after 15 rGO-coating cycles, corresponding to an add-on weight of $7.3 (\pm 0.99) \mu\text{g}$. Previous studies reported rGO add-on weight percent on woven cotton fabric of 3.31% with 15 coating cycles of immersion in a $2.25 \text{ wt}\%$ GO solution concentration [29]. The higher add-on ratio observed in our study may be due to the difference in the GO content in the coating solution, which was $4 \text{ wt}\%$ in our study.

The inset in Fig. 6 shows the R_s values of the corresponding rGO coating at the 5th, 10th, and 15th dipping obtained with the added exfoliation step included in the coating cycles. The resistance values observed for a given number of cycles are much higher than for the same number of cycles without exfoliation (Fig. 3). This can be attributed to the fact that exfoliation removed the extra rGO sheets loosely deposited over the fabric surface, leaving only a coating around the

individual fibers. Even if the exfoliation process leads to a decrease in conductivity of the rGO track, it is essential to ensure that the fabric normal use conditions (folding, bending, etc.) do not affect the electrical performance due to the presence of loosely bonded rGO sheets.

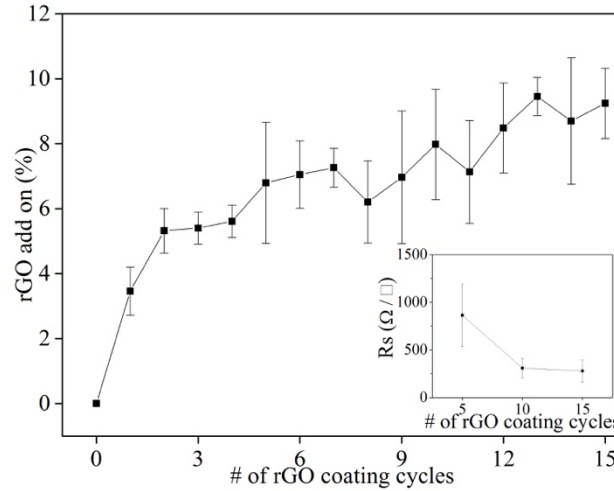


Fig. 6 Variation in the rGO add-on as a function of the number of rGO cycles for the as-received m-aramid fabric (where the exfoliation step was included between each coating cycle) (Inset: sheet resistance (R_s) versus the number of rGO cycles)

3.2 Washing fastness

One of the greatest challenges for a textile-based sensor is related to launderability. The mechanical stresses applied during the washing process may destroy the electrical interconnects [30]. The presence of water, high temperature and detergent chemicals may also affect textile-based sensors, particularly if the sensors cannot be coated by a protective layer without affecting their function (as is the case for our devices). In order to investigate the washing resistance of the rGO-coated meta-aramid fabric, the R_s of rGO-coated textiles was characterized after selected numbers of washing cycles. As shown in Fig. 7, the average R_s of the rGO-coated m-aramid textile with 5 rGO coating cycles (including the exfoliation step) was $863 (\pm 179) \text{ k}\Omega/\square$ before washing, and increased to $1.3 (\pm 0.4) \text{ M}\Omega/\square$ after 10 washing cycles. On the other hand, the R_s values of the samples that underwent 10 and 15 coating cycles increased by only 3.3% and 11.2%,

respectively, after 10 washing cycles. An ANOVA was performed on the data. The results of the ANOVA identify no statistical difference in R_s between the number of washing cycles for samples with 10 and 15 rGO coating cycles, with p-values of 0.16, and 0.29 respectively. On the other hand, for samples with 5 rGO coating cycles, the p-value is 7.68×10^{-6} , which points to statistical differences in R_s between the washing cycles. This implies that 5 rGO coating cycles are not enough to obtain stable electrical conductivity, and a minimum of 10 rGO coating cycles is required if that the rGO-coating on the m-aramid fabric will endure at least 50 domestic laundering cycles without a significant loss in electrical conductivity.

Fig. 8 and Fig. 9 show FE-SEM images of fabric samples prepared with 5 and 15 rGO coatings, both before washing and after 1, 5, and 10 washing cycle(s). For samples prepared with 5 rGO coating cycles (Fig. 8 (a) to (d)), the rGO coated layer on m-aramid fabric became cracked as the number of washing cycles increased. It is possible to see some rGO sheets partially peeling away from the fibers after 10 washing cycles (Fig. 8d). This failure of the rGO fiber covering explains the increase in the electrical resistance with the number of washing cycles for the 5 rGO coated samples that was observed in Fig. 7. On the other hand, for samples prepared using 15 rGO coating cycles (Fig. 9 (a) to (d)), no signs of cracking or delamination are observed, and the rGO sheets remain wrapped around the fibers. This observation is in agreement with the stable resistance recorded for up to 10 washing cycles.

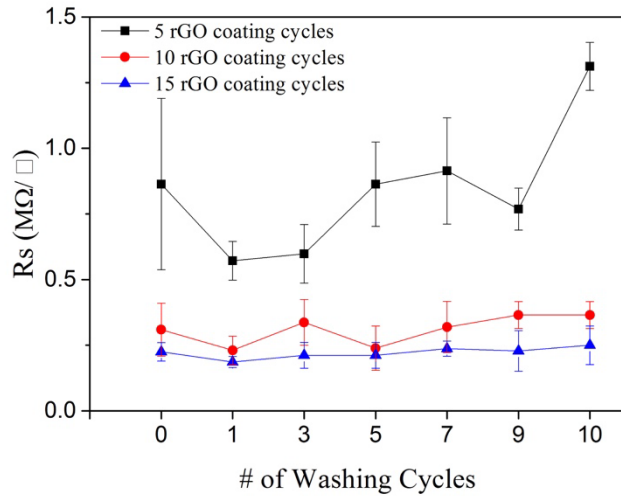


Fig. 7 Effect of up to 10 accelerated washing cycles on the sheet resistance (R_s) of m-aramid fabric with 5, 10, and 15 rGO coatings

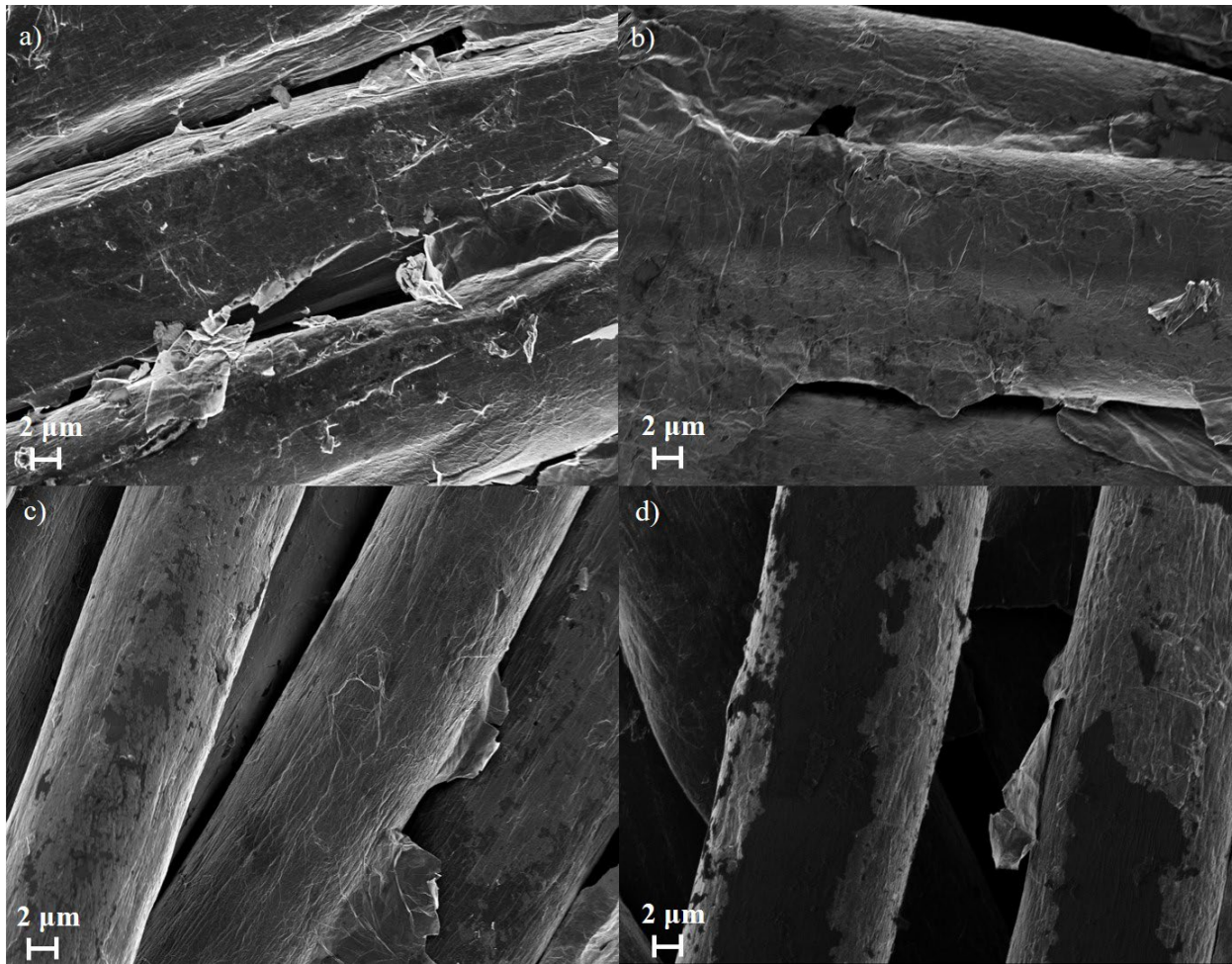


Fig. 8 FE-SEM images of m-aramid fabric with 5 rGO coatings on m-aramid textile a) before washing, b) after 1, c) 5, and d) 10 accelerated washing cycles.

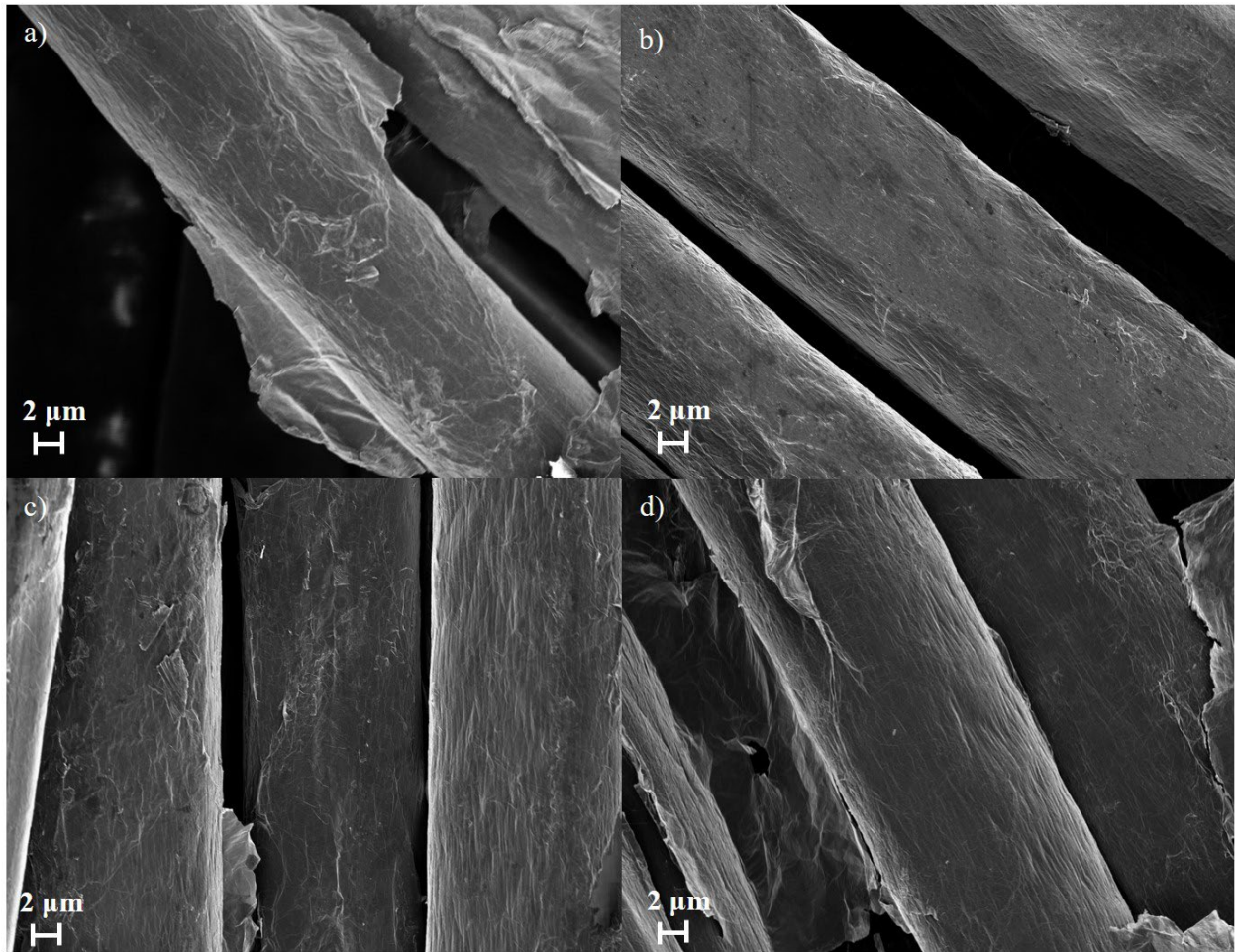


Fig. 9 FE-SEM images of m-aramid fabric with 15 rGO coatings on m-aramid a) before washing, b) after 1, c) 5, and d) 10 accelerated washing cycles.

3.3 Stability of the rGO coating upon water exposure

During use, fire-resistant fabrics may be exposed to varying sources of humidity including rainy environments, the wearer's perspiration, and immersion in water. One mechanism by which water can swell fibers is by generating voids and microcracks at the fiber-matrix interface [31-32]. Therefore, conductive traces on fabrics may be damaged when the textiles are exposed to water.

In order to study the rGO coating stability under water exposure, we immersed $2\text{ cm} \times 2\text{ cm}$, 15 rGO-coated m-aramid fabric specimens in water for up to 5 days, and the electrical resistance of the fabric was measured every 24 h. Fig. 10 shows the R_s value of the specimens

measured after each 24 h period. Differences in R_s measured after each 24 h period of immersion in water were not statically significant (with a p-value of 0.73).

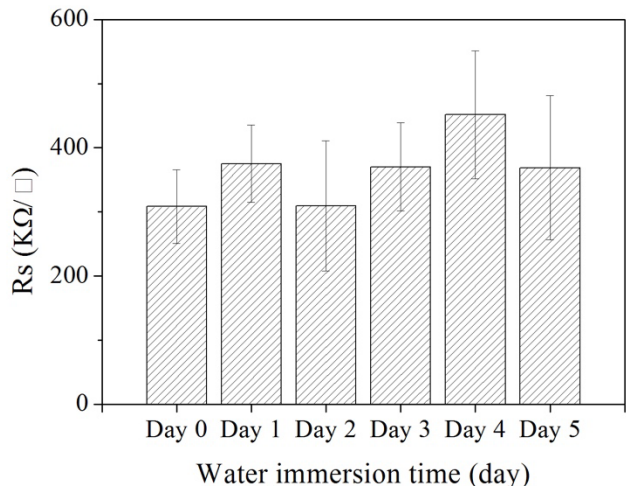


Fig. 10 Variation in the sheet resistance of 15th time rGO-coated fabric as a function of immersion time in water

The moisture regain of meta-aramid fibers at 65% relative humidity and 21°C (standard conditions for textile testing) is reported to be 4.5% (by weight) [33]. In addition, a technical sheet on m-aramid paper reports that – as a result of moisture vapour absorption under 96% relative humidity at room temperature – the m-aramid fibers expand approximately 1%, 2.5% and 4% in the warp direction, the weft direction, and the thickness, respectively [34]. However, a close look at Fig. 5 reveals that the rGO coating on m-aramid fibers is rather scaly and that some free volume exists between the graphene layer and the fiber. The graphene sheets may also have the ability to slide relative to each other and accommodate the limited swelling of the aramid fibers upon water immersion. This may explain in part why the rGO coating layer was able to maintain its electrical conductivity after water immersion for up to 5 days. In addition, the hydrophobic nature of the rGO coating may limit water adsorption on the fiber surface.

3.4 Resistance to abrasion

Abrasion resistance is an ability of textile materials to resist contact rubbing or surface wear. Thus, abrasion testing is an important assessment to predict the behavior of textiles in real life conditions [35]. In order to characterize the abrasion resistance of rGO-coating on m-aramid fabric, a coating procedure was developed to prepare rGO tracks on the m-aramid fabric (section 2.3). The abrasion testing was conducted in accordance with ASTM D4966 [28], using the methodology described in section 2.6.

Each specimen was patterned with three parallel, rectangular rGO tracks. The abrasion tester has discs of worsted wool abradant, and these discs rub the specimen with a trajectory of Lissajour curve [36]; in other words, the center part of the specimen is more frequently abraded compared to the peripheral parts. As a result, the resistance of the center rGO track increased more quickly than those of the top and the bottom ones. Fig. 11 (a) shows the variation in electrical resistance as a function of the number of abrading cycles for rGO tracks deposited on one side of the fabric. The resistance gradually increased with the number of abrasion cycles until it reached 150 cycles. Afterwards, the resistance jumped abruptly out of the instrument range (measuring up to 60 M Ω , corresponding to 1 M Ω/\square in R_s), which indicated that the electrical conductivity was completely lost. Fig. 11(a) also shows that above 50 cycles, a marked difference in conductivity loss occurs between the track situated in the center of the specimen and the two tracks on each side. This is attributed to the inhomogeneous pressure distribution across the abrasion sample holder surface area created by the foam padding between the sample holder and the specimen. Below 50 abrasion cycles, the high resistance measurement variability prevents distinguishing between the behavior of the three tracks.

As an alternative approach to maintain electrical conduction against rGO loss from abrasion, tracks were formed on both sides of the fabric. The protocol developed (Section 2.3) ensured that the tracks on one face of the fabric were exactly superimposed over the tracks on the opposite face. Fig. 11 (b) shows that the two-sided rGO tracks undergo a moderate decrease in electrical conductivity with increasing number of abrasion cycles, but the rate is much lower compared to the single-sided rGO tracks: the resistance increase was less than a decade over 3000 abrasion cycles as compared with an increase of over two decades after only 150 cycles. This can be attributed to the almost complete penetration of the rGO coating through the fabric thickness as evidenced by the HIM cross section image of the two-sided rGO tracks shown in Fig. 12. The difference in the abrasion rate on the loss of electrical conductivity between the center track and the tracks on each side (labelled top and bottom) can also be observed in Fig. 11 (b). After 3000 abrasion cycles, the electrical resistance of the center track underwent 10-fold increase while those of the two other tracks increased by ~ 4 times.

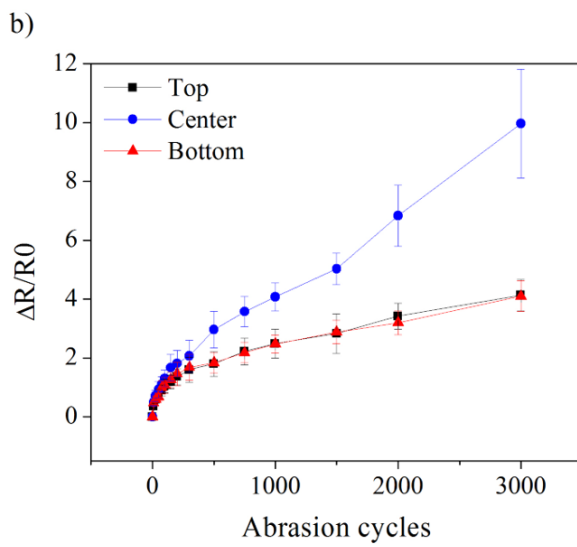
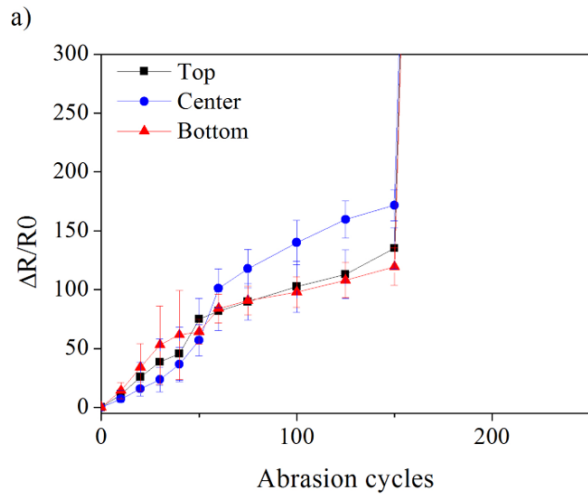


Fig. 11 Influence of Martindale abrasion on resistance of a) single-sided rGO tracks, and b) double-sided rGO tracks. (Top, center, and bottom labels correspond to the location of the three tracks on the specimen).

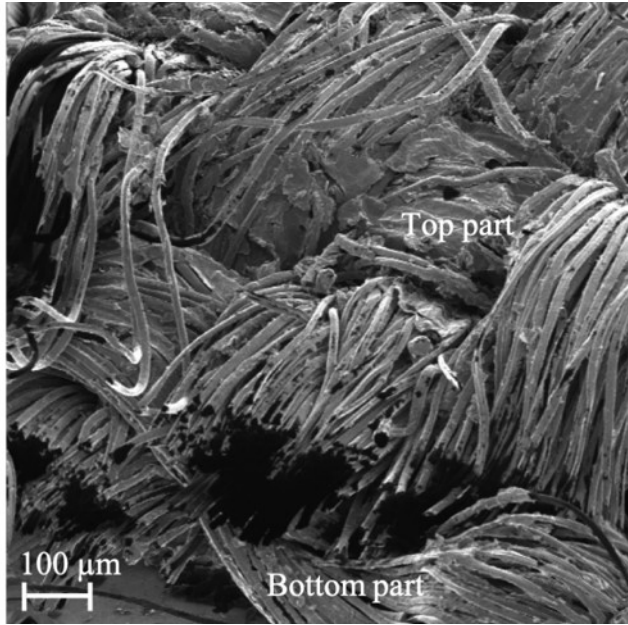


Fig. 12 Bird's eye view (54° tilting) on the cross-sectional area of the m-aramid fabric sample with two-sided rGO tracks (top and bottom fabric parts are indicated; insulated area appears solid black). Helium Ion Microscopy (HIM) was used for imaging.

4. Conclusions

The objective of the present work with an m-aramid woven fabric was to establish a protocol of stable rGO coating that loses its conductivity by controlled abrasion. The underlying motivation of this study is to apply the stable rGO coating with controlled conductivity loss as a platform for an end-of-life sensor for high-performance textiles. In order to achieve the stable rGO coating, up to 15 iterations of “dip and dry” method was applied with exfoliation step at the end of each cycle. This wrapped rGO coating did not show any sign of degradation in conductivity under 10 accelerated washing cycles (equivalent to 50 domestic washing cycles) and under water immersion (up to 5 days). Under abrasion cycles, on the other hand, a systematic degradation behavior was observed.

Another point to highlight is our heat-pressure-transfer protocol of wax printed patterns. This simple technique allows selective coating of rGO on fabric to form high fidelity patterns, whereas the pattern can simply be fabricated by a commercial desktop wax printer.

In future studies, we envision that our rGO patterning technique can be used to prepare an aging indicator for high-performance fabrics such as m-aramid. These laundering and abrasion behavior of these rGO tracks can be tailored to match the requirements of the sensor design; this opens large opportunities for the application of graphenic nanomaterials as end-of-life sensors.

Acknowledgements

We acknowledge the NSERC Strategic Project Grant (SPG) STPGP 521866 for financial support of this work. We thank Syed Asad Manzoor Bukhari for his help in HIM imaging. Material characterization was partly done in the shared facility of the NanoFAB in the Faculty of Engineering at the University of Alberta.

Compliance with ethical standards

Conflict of interest: The authors declare that there is no conflict of interest regarding the publication of this paper.

References

- [1] R. Nayak, S. Houshyar, and R. Padhye, "Recent trends and future scope in the protection and comfort of fire-fighters' personal protective clothing," *Fire Sci. Rev.*, vol. 3, no. 1, p. 4, 2014.
- [2] M. McQuerry, S. Klausning, D. Cotterill, and E. Easter, "A Post-use Evaluation of Turnout Gear Using NFPA 1971 Standard on Protective Ensembles for Structural Fire Fighting and NFPA 1851 on Selection, Care and Maintenance," *Fire Technol.*, 2015.
- [3] C. Arrieta, E. David, P. Dolez, and T. Vu-Khanh, "Thermal aging of a blend of high-performance fibers," *J. Appl. Polym. Sci.*, vol. 115, no. 5, pp. 3031–3039, Oct. 2009.
- [4] R. M. Rossi, W. Bolli, and R. Stämpfli, "Performance of Firefighters' Protective Clothing After Heat Exposure," *Int. J. Occup. Saf. Ergon.*, vol. 14, no. 1, pp. 55–60, Jan. 2008.
- [5] M. Day, J. D. Cooney, and T. Suprunchuk, "Durability of Firefighters' Protective Clothing to Heat and Light," *Text. Res. J.*, vol. 58, no. 3, pp. 141–147, Mar. 1988.
- [6] C. Arrieta, É. David, P. Dolez, and T. Vu-Khanh, "Hydrolytic and photochemical aging studies of a Kevlar®-PBI blend," *Polym. Degrad. Stab.*, vol. 96, no. 8, pp. 1411–1419, 2011.
- [7] M. Rezaadeh and D. A. Torvi, "Assessment of Factors Affecting the Continuing Performance of Firefighters' Protective Clothing: A Literature Review," *Fire Technol.*, vol. 47, no. 3, pp. 565–599, 2011.
- [8] M. Fulton, M. Rezaadeh, and D. Torvi, "Tests for evaluating textile aging," *Adv. Charact. Test. Text.*, pp. 93–125, Jan. 2018.
- [9] L. M. Castano and A. B. Flatau, "Smart fabric sensors and e-textile technologies: A review," *Smart Mater. Struct.*, vol. 23, no. 5, 2014.

- [10] K. Krishnamoorthy, U. Navaneethaiyer, R. Mohan, J. Lee, and S.-J. Kim, "Graphene oxide nanostructures modified multifunctional cotton fabrics," *Appl. Nanosci.*, vol. 2, no. 2, pp. 119–126, 2012.
- [11] J. Molina, J. Fernández, J. C. Inés, A. I. del Río, J. Bonastre, and F. Cases, "Electrochemical characterization of reduced graphene oxide-coated polyester fabrics," *Electrochim. Acta*, vol. 93, pp. 44–52, 2013.
- [12] M. Shateri-Khalilabad and M. E. Yazdanshenas, "Preparation of superhydrophobic electroconductive graphene-coated cotton cellulose," *Cellulose*, vol. 20, no. 2, pp. 963–972, 2013.
- [13] M. Stoppa and A. Chiolerio, "Wearable electronics and smart textiles: A critical review," *Sensors (Switzerland)*, vol. 14, no. 7, pp. 11957–11992, 2014.
- [14] M. Shateri-Khalilabad and M. E. Yazdanshenas, "Fabricating electroconductive cotton textiles using graphene," *Carbohydr. Polym.*, vol. 96, no. 1, pp. 190–195, Jul. 2013.
- [15] N. Karim et al., "All Inkjet-printed Graphene-based Conductive Pattern for Wearable E-textiles Application," *J. Mater. Chem. C*, 2017.
- [16] G. D. Mura et al., "Piezoresistive goniometer network for sensing gloves," in *IFMBE Proceedings*, 2014.
- [17] J. Mikkonen and E. Pouta, "Flexible Wire-Component for Weaving Electronic Textiles," in *2016 IEEE 66th Electronic Components and Technology Conference (ECTC)*, 2016, pp. 1656–1663.
- [18] L. Shu, T. Hua, Y. Wang, Q. Qiao Li, D. D. Feng, and X. Tao, "In-shoe plantar pressure measurement and analysis system based on fabric pressure sensing array.," *IEEE Trans. Inf. Technol. Biomed.*, 2010.
- [19] J. A. Rogers, T. Someya, and Y. Huang, "Materials and mechanics for stretchable electronics," *Science*. 2010.
- [20] C. Gonçalves, A. Ferreira da Silva, J. Gomes, and R. Simoes, "Wearable E-Textile Technologies: A Review on Sensors, Actuators and Control Elements," *Inventions*, vol. 3, no. 1, p. 14, 2018.
- [21] A. Chatterjee, M. Nivas Kumar, and S. Maity, "Influence of graphene oxide concentration and dipping cycles on electrical conductivity of coated cotton textiles," *J. Text. Inst.*, vol. 108, no. 11, pp. 1910–1916, 2017.
- [22] S. He, B. Xin, Z. Chen, and Y. Liu, "Flexible and highly conductive Ag/G-coated cotton fabric based on graphene dipping and silver magnetron sputtering," *Cellulose*, vol. 25, no. 6, pp. 3691–3701, Jun. 2018.
- [23] H. Lee et al., "Preparation of fabric strain sensor based on graphene for human motion monitoring," *J. Mater. Sci.*, vol. 53, no. 12, pp. 1–8, 2018.
- [24] X. Li, Y. Chen, A. Kumar, A. Mahmoud, J. A. Nychka, and H. J. Chung, "Sponge-Templated Macroporous Graphene Network for Piezoelectric ZnO Nanogenerator," *ACS Appl. Mater. Interfaces*, vol. 7, no. 37, pp. 20753–20760, 2015.
- [25] Y.A. Samad, Y. Li, S.M. Alhassan, and K. Liao, "Non-destroyable graphene cladding on a range of textile and other fibers and fiber mats" *RSC Advances*, vol. 4, no. 33, pp. 16935-16938, 2014.
- [26] "CAN/CGSB-4.2 No. 58-2004 Textile Test Methods - Dimensional Change in Domestic Laundering of Textiles."
- [27] ISO 105-C06, "ISO Textiles - test for color fastness - part C06: Colour Fastness to Domestic and Commercial Laundering," 2010.

- [28] ASTM D-4966, “Standard Test Method for Abrasion Resistance of Textile Fabrics (Martindale Abrasion,” 2015.
- [29] E. Menezes and M. Choudhari, “Pre-treatment of textiles prior to dyeing,” *Text. Dye.*, pp. 221–241, 2011.
- [30] R. Pramod and M. E. Shashi Kumar, “Evaluation of mechanical and insulation properties of nomex-T410 and HS glass polymer matrix composites,” *Mater. Today Proc.*, vol. 4, no. 2, pp. 3233–3242, 2017.
- [31] X. Tao, V. Koncar, T. H. Huang, C. L. Shen, Y. C. Ko, and G. T. Jou, “How to make reliable, washable, and wearable textronic devices,” *Sensors (Switzerland)*, vol. 17, no. 4, 2017.
- [32] T. Alomayri, H. Assaedi, F. U. A. Shaikh, and I. M. Low, “Effect of water absorption on the mechanical properties of cotton fabric-reinforced geopolymer composites,” *J. Asian Ceram. Soc.*, vol. 2, no. 3, pp. 223–230, 2014.
- [33] B. J. Collier, M. J. Bide, and P. G. Tortora, *Understanding textiles*, 7th ed. Upper Saddle River, N.J.: Pearson Prentice Hall, 2009.
- [34] Dupont®, “Moisture Effects and Processing Information for Nomex ® Paper Perform When the Heat’s on.”
- [35] N. Özdil, G. Ö. Kayseri, and G. S. Mengüç, “Analysis of abrasion characteristics in textiles,” *Abrasion Resist. Mater.*, pp. 119–146, 2008.
- [36] L. Sabantina, F. Kinzel, A. Ehrmann, and K. Finsterbusch, “Combining 3D printed forms with textile structures - mechanical and geometrical properties of multi-material systems,” *IOP Conf. Ser. Mater. Sci. Eng.*, vol. 87, p. 012005, Jul. 2015.